Hindawi Publishing Corporation
EURASIP Journal on Wireless Communications and Networking
Volume 2007, Article ID 49718, 17 pages
doi:10.1155/2007/49718

Research Article

Advanced Fade Countermeasures for DVB-S2 Systems in Railway Scenarios

Stefano Cioni,[1] Cristina Párraga Niebla,[2] Gonzalo Seco Granados,[3] Sandro Scalise,[2] Alessandro Vanelli-Coralli,[1] and María Angeles Vázquez Castro[3]

[1] *ARCES, University of Bologna, Via Toffano 2, 40125 Bologna, Italy*
[2] *German Aerospace Center (DLR), Institute of Communications and Navigation, Postfach 1116, 82230 Wessling, Germany*
[3] *Department of Telecommunications and Systems Engineering, Universitat Autònoma de Barcelona, Campus Universitari, s/n, 08193 Bellatera, Barcelona, Spain*

Received 22 October 2006; Accepted 3 June 2007

Recommended by Ray E. Sheriff

This paper deals with the analysis of advanced fade countermeasures for supporting DVB-S2 reception by mobile terminals mounted on high-speed trains. Recent market studies indicate this as a potential profitable market for satellite communications, provided that integration with wireless terrestrial networks can be implemented to bridge the satellite connectivity inside railway tunnels and large train stations. In turn, the satellite can typically offer the coverage of around 80% of the railway path with existing space infrastructure. This piece of work, representing the first step of a wider study, is focusing on the modifications which may be required in the DVB-S2 standard (to be employed in the forward link) in order to achieve reliable reception in a challenging environment such as the railway one. Modifications have been devised trying to minimize the impact on the existing air interface, standardized for fixed terminals.

1. INTRODUCTION

Satellite communications developed to a tremendous global success in the field of analog and then digital audio/TV broadcasting by exploiting the inherent wide-area coverage for the distribution of content. It appeared a "natural" consequence to extend the satellite services for point-to-point multimedia applications, by taking advantage of the ability of satellite to efficiently distribute multimedia information over very large geographical areas and of the existing/potential large available bandwidth in the Ku/Ka band. Particularly in Europe, due to the successful introduction of digital video broadcasting via satellite (DVB-S) [1], a promising technical fundament has been laid for the development of satellite communications into these new market opportunities using the second generation of DVB-S [2], commonly referred to as DVB-S2, as well as return channel via satellite (DVB-RCS) [3] standards. Thus, for satellite systems currently under development and being designed to support mainly multimedia services, the application of the DVB-S2, for the high-capacity gateway-to-user (forward) links and of DVB-RCS for the user-to-gateway (return) links, is widely accepted.

Complementing to satellite multimedia to fixed terminals, people are getting more and more used to broadband communications on the move. Mobile telephones subscriptions have exceeded fixed line subscription in many countries. Higher data rates for mobile devices are provided by new standards such as UMTS, high-speed packet access (HSPA), prestandardized version of mobile WiMAX, and, in case of broadcast applications, digital video broadcasting for handhelds (DVB-H) [5].

At present, broadband access (e.g., to the Internet) and dedicated point-to-point links (for professional services) are primarily supplied by terrestrial networks. Broadband satcoms services are still a niche market, especially for mobile users. In this context, many transport operators announce the provision of TV services in ships, trains, buses, and aircrafts. Furthermore, Internet access is offered to passengers. With IP connectivity, also radio interfaces for GSM can be implemented for such mobile platforms by using satellite connectivity for backhauling.

Thus, DVB-S2/RCS appears an ideal candidate to be investigated for mobile usage, as it can ideally combine digital TV broadcast reception in mobile environments (airTV, luxury yachts, trains, etc.) and IP multimedia services.

However, the aforementioned standards have not been designed for mobile use. Collective terminals installed in a mobile platform, such as train, ship, or aircraft, are exposed to a challenging environment that will impact the system performance considering the current standard in absence of any specific provision.

Mobile terminals will have to cope in general with stringent frequency regulations (especially in Ku band), Doppler effects, frequent handovers, and impairments in the synchronization acquisition and maintenance. Furthermore, the railway scenario is affected by shadowing and fast fading due to mobility, such as, for example, the deep and frequent fades due to the presence of metallic obstacles along electrified lines providing power to the locomotive[1] [6] and long blockages due to the presence of tunnels and large train stations. This suggests that hybrid networks, that is, interworking satellite and terrestrial components, are essential in order to keep service availability.

In this context, this paper is focused on proposing and evaluating fade countermeasures to compensate the impact of fade sources in the railway scenario, that is, shadowing, fast fading, and power arches, excluding tunnels which will be address at a later stage. In particular, antenna diversity and packet level forward error correction (FEC) are investigated.

The rest of the paper is organized as follows: Section 2 discusses the potential of opening the current DVB-S2/RCS standards to provide mobile services efficiently. Section 3 presents the peculiarities of the trains' scenario and discusses the different aspects that can impact the system performance. Section 4 describes the fade countermeasures proposed in this paper. Section 5 introduces the simulation platforms in which the proposed fade countermeasures are evaluated and Section 6 presents and discusses the obtained results. Finally, Section 7 draws the conclusions of this work.

2. THE VISION: A NEW DVB-S2/RCS STANDARD FOR MOBILE COLLECTIVE TERMINALS

The large capacity of DVB-S2/RCS systems can efficiently accommodate broadcast services (e.g., digital TV) and unicast IP multimedia interactive services to fixed terminals. However, the increasing interest on broadband mobile services suggests that the natural evolution of DVB-S2/RCS standard to cover new market needs goes towards the support of mobile terminals.

In particular, the required antenna performance in Ku (10–12 GHz) and Ka (20–30 GHz) bands focuses the market opportunities of DVB-S2/RCS onto mobile terminals in collective transportation means. Actually, transport operators are starting to announce the provision of TV services in ships, trains, buses, and aircrafts, and broadband IP connectivity, for passengers. For the specific case of trains, broadband services can provided using satellite systems, cellular connectivity or dedicated trackside installations.

As summarized in Table 1, none of these alternatives alone represents a satisfactory solution. As a matter of fact, deployed or upcoming commercial services are based on combinations of different access technologies. In this light, a satellite access based on an open standard can have very significant benefits in terms of interoperability (achieved for DVB-S2/RCS through SatLabs Qualification Program) and competition, thus benefiting from availability of fully compatible terminals from multiple vendors and reducing the cost of terminals.

However, the aforementioned DVB standards have been designed for fixed terminals. To cope with these new market opportunities, DVB TM-RCS has investigated how the current DVB-RCS standard could be applied to mobile applications. A white paper on the applicability of DVB-RCS to mobile services was prepared and a technical annex was added to the implementation guidelines document [4]. This annex states the boundary conditions and limitations under which the existing standard could be used in mobile environment, considering the impact of mobility in terminal synchronization and demodulator performance in forward and return links. Furthermore, a survey on applicable regulations and a brief analysis on DVB-RCS features that can be used for mobility management are provided, the latter referring to interbeam handover only.

Thus, the DVB-RCS guideline cannot support the full adaptability to mobile environments and hence the applicable services and scenarios happen to be very limited. Furthermore, additional issues related to mobility are not fully solved, such as handling of nonline-of-sight (nLOS) channel conditions, which will require the interworking with terrestrial gap fillers in the railway scenario due to the presence of tunnels. In addition, even if DVB-RCS features to be applied for mobility management are analyzed, a determined mechanism or protocol should be specified in order to ensure interoperability. Finally, the impact of control signals loss (due to deep fades or handover) is not negligible. For instance, the loss of terminal burst time plan (TBTP) tables damages the operation of the resource management, essential in the return link for a coordinated access to the radio resources.

As a matter of fact, mobile services could be more efficiently supported if the present standards could be improved for mobile scenarios. The reopening of the standard[2] would allow for the specification of methods for improving the link reliability in mobile environments (e.g., packet level FEC), handover protocols, interfaces to terrestrial gap fillers (even using terrestrial mobile technologies), improved mobility-aware signalling and resource management, and so forth.

In this context, a number of R and D initiatives are ongoing with the aim at investigating enhancements of the DVB-S2/RCS standards for the efficient support of mobility. Among those, the SatNEx network of excellence has set up a dedicated working group investigating different aspects related to mobility in DVB-S2/RCS. The first results of this activity in the field of forward link reliability for the railway scenario are presented in this paper. For the return link,

[1] Hereafter referred to as "power arches," for the sake of brevity.

[2] Envisaged at the time of writing.

Table 1: Pros and cons of different solutions for providing broadband services on trains.

Type of technology	Examples	Pros	Cons
Satellite	DVB-S2/RCS Proprietary systems, for example, ViaSat	(i) No new trackside infrastructure—quick to deploy, project costs may be lower on long distance routes	(i) Available tracking antennas and efficient satcom modems expensive
		(ii) Dedicated bandwidth available	(ii) High variable cost per MB
		(iii) Performance easy to predict depending on satellite visibility	(iii) Return bandwidth constrained by antenna size
		(iv) Not affected by borders—good for international trains	(iv) Satellite visibility seriously restricted on some rail routes
Cellular	GPRS EDGE UMTS HSUPA/HSDPA (EV-DO)	(i) Equipment is small and cheap	(i) Geographic coverage of UMTS limited for years to come
		(ii) Usage is cheap (50–75 € per month flat rate)	(ii) Coverage of railway lines often worse than roads
		(iii) Data rates improving year on year	(iii) GPRS/EDGE not really fast enough
		(iv) Competitive supply—3 or 4 network operators in most countries	(iv) Inverse relationship between throughput and train speed
			(v) No QoS guarantees—affected by network congestion at peak times
			(vi) Organized country by country—data roaming charges are punitive
Trackside	Flash OFDM IEEE 802.11 IEEE 802.16 (WiMAX)	(i) High data rates possible	(i) Existing standards not designed to support fast-moving terminals
		(ii) Can control bandwidth and QoS	(ii) Proprietary equipment is more expensive
		(iii) On-train equipment relatively inexpensive	(iii) No suitable public services yet in licensed bands—will licence-holders be allowed to provide mobile services?
		(iv) No volume-related usage costs	(iv) Licence-exempt bands are low power, thus limited range
			(v) Infrastructure deployment (especially trackside) is expensive and time consuming

analogue solutions have to be devised, which are however not in the scope of the present work.

3. THE RAILWAY SCENARIO, A CHALLENGING ENVIRONMENT

3.1. Overview

The land mobile satellite channel (LMSC) has been widely studied in the literature [7]. Several measurement campaigns have been carried out and several narrow and wideband models have been proposed for a wide range of frequencies, including Ku [8] and Ka [9] bands. Nevertheless, for the specific case of the railway environment, only few results are presented in [10] as a consequence of a limited trial campaign using a narrowband test signal at 1.5 GHz, performed more than 10 years ago in the north of Spain. These results represent a very interesting reference, although no specific channel model has been extracted from the collected data. After an initial qualitative analysis, the railway environment appears to differ substantially with respect to the scenarios normally considered when modelling the LMSC. Excluding railway tunnels and areas in the proximity of large railway stations, one has to consider the presence of several metallic obstacles like power arches (Figure 1, left uppermost), posts with horizontal brackets (Figure 1, left lowermost), which may be often grouped together (Figure 1, rightmost), and catenaries, that is, electrical cables, visible in all the aforementioned figures.

The results of direct measurements performed along the Italian railway and aiming to characterize these peculiar obstacles are reported in [6] and references herein. In summary,

Figure 1: Nomenclature of railway specific obstacles.

the attenuation introduced by the catenaries (less than 2 dB) and by posts with brackets (2-3 dB) is relatively low and can be easily compensated by an adequate link margin. On the other hand, the attenuation introduced by the power arches goes, depending on the geometry, the radiation pattern of the RX antenna, and the carrier frequency, down to values much greater than 10 dB.

3.2. Modelling

Even if the layout and exact geometry of such obstacles can significantly change depending on the considered railway path, it turned out from previous works that the attenuation introduced by these kind of obstacles can be accurately modelled using knife-edge diffraction theory [11]: in presence of an obstacle having one infinite dimension (e.g., mountains or high buildings), the knife-edge attenuation can be computed as the ratio between the received field in presence of the obstacle and the received field in free space conditions. In the case addressed here, as shown in Figure 2 (left), the obstacle has two finite dimensions, and the received field is hence the sum of the contributions coming from both sides of the obstacle. Therefore, the resulting attenuation can be written as follows:

$$A_s(h) = \frac{1}{\sqrt{2}G_{\max}}\left(G(\alpha_1(h))\left|\int_{Kh}^{\infty} e^{-j(\pi/2)v^2}dv\right| + G(\alpha_2(h))\left|\int_{-\infty}^{K(h-d)} e^{-j(\pi/2)v^2}dv\right|\right), \quad (1)$$

$$K = \sqrt{\frac{2}{\lambda}\frac{a+b}{a\cdot b}},$$

where λ is the wavelength, a is the distance between the receiving antenna and the obstacle, b is the distance between the obstacle and the satellite, h is the height of the obstacle above the line-of-sight (LOS), and d is the width of the obstacle. Finally, the usage of a directive antenna with radiation pattern $G(\alpha)$ has to be considered. This implies an additional attenuation due to the fact that whenever the two diffracted rays reach the receiving antenna with angles α_1 and α_2 as shown in Figure 2(left), the antenna shows a gain less than the maximum achievable ($G_{\max}$) and depending on the variable h, which is directly related to the space covered by the train.

In absence of a channel model directly extracted from measurements in the railway environment, it is a common practice to model the so-called "railroad satellite channel" by superimposing (i.e., multiplying) the statistical fades reproduced by a Markov model (see [8, 9]) with the space-periodic fades introduced by the electrical trellises obtainable by means of the above equation. Values of the parameters in Figure 2, as well as the space separation between subsequent electrical trellises, depend on the considered railway. Finally, the considered receiving antennas are modelled with high directivity in order to achieve large gain and at the same time to reduce the received multipath components with large angular spread. Hence, as reported in [12], the key parameter becomes the antenna beamwidth which describes in the frequency domain the Doppler power spectrum density of the satellite fading channel. In this paper, the highly directive antennas are modelled with the reasonable value of the beamwidth in the order of 5 degrees.

3.3. Need for fade countermeasures and gap fillers

The periodical fading events induced by power arches (PA) result in a physical error floor that limits the performance of the DVB-S2 system to unacceptable quality of service (QoS) levels. In Figure 3, the baseband frame (BBFRAME) error rate is reported in LOS conditions, for train speed equal to 300 km/h, and in the presence of power arches, when the receiver has only one receiving antenna and does not adopt any packet level FEC technique. The error floor value is about 0.0117, corresponding to the ratio between the duration of PA induced fading events, that is, 6 msilliseconds at 300 km/h, and the time between two fading events, that is, 600 msilliseconds at 300 km/h. Considering the case of 27.5 Mbaud, the DVB-S2 BBFRAME duration is less than 1 msillisecond, therefore when the receiving antenna is obscured by a power arch, transmitted packets are completely lost unless fade countermeasures are adopted.

4. ADVANCED FADE COUNTERMEASURES

System designers can resort to different approaches to counteract deep fading conditions and to guarantee an acceptable QoS level. A possible classification of fade countermeasure is between those techniques that need a return channel (from the user to the network) to require a change in the transmission mode or a retransmission of the lost information, and those that do not rely on a return channel and are therefore more suitable for unidirectional delivery, such as multicast or broadcast applications. The latter class of techniques is of great interest for the collective railway application considered in this work, for which return channel-based approaches, such as automatic repeat request (ARQ) or adaptive coding and modulation (ACM) techniques, are not doable. In particular, antenna diversity and packet level FEC techniques are considered in the following.

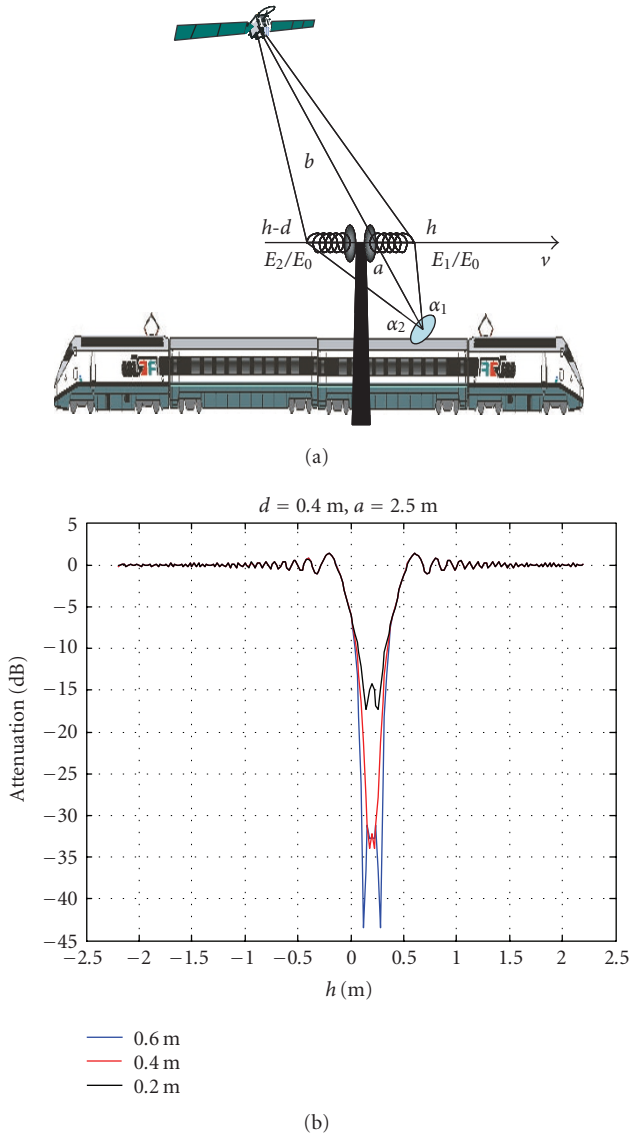

Figure 2: Knife-edge diffraction model applied to the railway scenario and possible attenuation caused by power arches at Ku band for different antenna diameters.

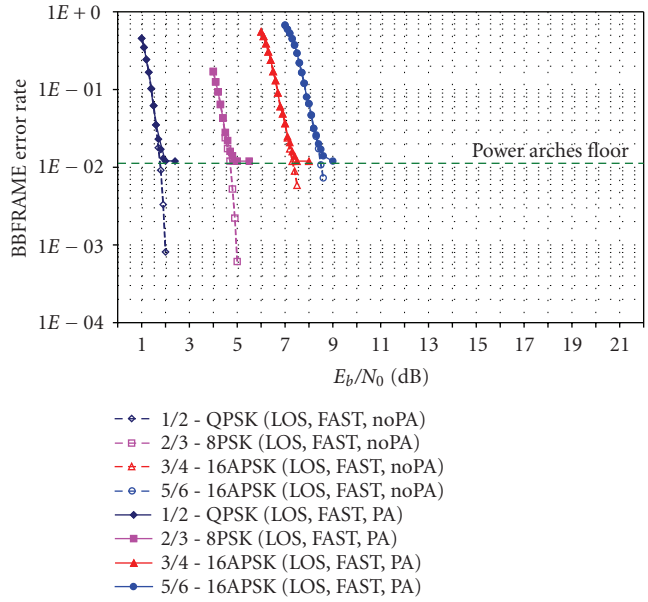

Figure 3: BBFRAME error rate for DVB-S2 in the presence of power arch blockage events. LOS propagation conditions and train speed set to 300 km/h.

4.1. Antenna diversity

The adoption of multiple receiving antennas to counteract power arch obstructions in railway environment has been recently proposed and investigated in [13, 14]. Antenna diversity is used to provide different replica of the received signal to the detector for combination or selection. If the receiving antennas are sufficiently spaced, the received signals fade independently on each antenna thus providing multiple diversity branches that can be linearly or nonlinearly combined to improve detection reliability. There are mainly three types of linear diversity combining approaches: selection, maximal-ratio, and equal-gain combining. Considering two receiving antennas, and assuming perfect compensation of time delays of the two replicas, the combined signal can be written as

$$r_c(t) = w_1 r_1(t) + w_2 r_2(t), \tag{2}$$

where w_i and $r_i(t)$, $i = 1, 2$, are the combing weights and the received signals, respectively. The received signals at each antenna is

$$r_i(t) = \alpha_i s_0(t) + n_i(t), \tag{3}$$

where $s_0(t)$ is the transmitted signal, α_i is the time variant fading envelope over the ith antenna, and $n_i(t)$ is the thermal noise.

The simplest combining scheme is the signal selection Combining (SC), in which the branch-signal with the largest amplitude or signal-to-noise ratio (SNR) is the one selected for demodulation. In this case, w_i will be 1 or 0 if the ith power branch is the largest or the smallest, respectively. Clearly, SC is bounded by the performance of the single receiving antenna in absence of fading, that is, there is no diversity gain when the two antennas experience good channel conditions at the same time. Maximum-ratio combining (MRC), although requiring a larger complexity at the receiver, allows for the exploitation of the diversity gain. In fact, MRC scheme provides for the maximum output SNR. According to the optimum combination criterion, the signal weights are directly proportional to the fading amplitude and inversely proportional to the noise power, N_i, as follows:

$$w_i = \frac{\alpha_i}{N_i}. \tag{4}$$

Another technique, often used because it does not require channel fading strength estimation, is equal gain combining

(EGC) in which the combination weights are all set to one, thus leading to a simpler but suboptimal approach. Clearly, SC and MRC (or EGC) represent the two extremes in diversity combining strategy with respect to the complexity point of view and the number of signals used for demodulation process. Furthermore, the classical combining formula can be generalized for nonconstant envelope modulations such as 16-APSK or 32-APSK (amplitude and phase shift keying) and integrated with the soft demodulator that computes the channel a posteriori information to feed the low density parity check (LDPC) FEC decoder. The maximum likelihood a priori information for a single receiver antenna given by

$$\log\left(\frac{\Pr\{b_i = 0 \mid r_k\}}{\Pr\{b_i = 1 \mid r_k\}}\right) = \log\left(\frac{\sum_{s_i \in S_0} \exp\left(-\left|r_k - \hat{\alpha}_k s_i\right|^2 / N_0\right)}{\sum_{s_i \in S_1} \exp\left(-\left|r_k - \hat{\alpha}_k s_i\right|^2 / N_0\right)}\right) \tag{5}$$

can be extended for L receiving antennas, according to the MRC principle, as follows:

$$\log\left(\frac{\Pr\{b_i = 0 \mid r_k\}}{\Pr\{b_i = 1 \mid r_k\}}\right) = \log\left(\frac{\sum_{s_i \in S_0} \exp\left(-\sum_{p=0}^{L}\left(\left|r_k^p - \hat{\alpha}_k^p s_i\right|^2 / N_0^p\right)\right)}{\sum_{s_i \in S_1} \exp\left(-\sum_{p=0}^{L}\left(\left|r_k^p - \hat{\alpha}_k^p s_i\right|^2 / N_0^p\right)\right)}\right), \tag{6}$$

where r_k is the received sample at time k, $\hat{\alpha}_k$ is the true or the estimated channel coefficient, and S_0 and S_1 are the sets of symbols which have "0" or "1" in the ith position, respectively.

In the configuration proposed in this work, we adopt MRC combining with two antennas. The antennas are placed on the same coach so as to reduce the costs of installation and the connection length. The antenna spacing is chosen as a function of the distance between two consecutive power arches so as to guarantee that only one antenna at a time can be obscured. Accordingly, the distance between the two antennas is about 15 m. Considering the maximum train speed (about 300 km/h), this translates into the fact that power-arch blockage on a single antenna lasts for about 7 msilliseconds, and it hits the second antenna after about 180 msilliseconds. Therefore, it is reasonable to assume that there is enough time for the combining circuit to react and maintain constant signal connection. A drawback of this approach is that the receiving chain will be duplicated in order to maintain connection and avoid frequent reacquisitions process with the consequent loss of packet. As proposed in [14], the solution which considers the presence of a second receiving antenna is depicted in Figure 4. The gray blocks represent the subsystems that need to be duplicated in the two antenna case. Further details on the digital receiver are described in Section 5.1.

4.2. Packet level FEC

4.2.1. The concept of packet level FEC

Reliable transmission occurs when all recipients correctly receive the transmitted data. This target can be achieved by operating at different layers of the protocol stack and in different ways. Retransmission techniques allow that lost packets are retransmitted to the receivers, while packet level FEC schemes create redundant packets that permit to reconstruct the lost ones at the receiver side, with a very beneficial input on the final end-to-end delay. In fact, as detailed in [15], the additional delay introduced by packet level encoding and decoding is always lower than the delay deriving from any retransmission scheme.

Regarding the retransmission schemes, efficient protocols should limit the use of acknowledgement- (ACK-) based mechanisms because they introduce heavy feedback traffic towards the sender, thus increasing the congestion of reverse link that, typically, has a reduced capacity with respect to forward link. Negative acknowledgement- (NACK-) based approaches are hence particularly interesting. In combination with (or in alternative to) the traditional retransmission schemes, packet level FEC can be added on top of physical layer FEC, in order to achieve the same level of reliability with a reduced number of retransmissions. This might be particularly useful if resources on the return link need to be saved (smaller number of NACKs or no NACKs are needed at all), or when multiple lost packets are recovered with the retransmission of a lower number of redundant packets. Basically, h redundancy packets are added to each group of k information packets, thus resulting in the transmission of $n = k + h$ packets. These packets are finally transferred to the physical layer, which adds independent channel coding to each of them. This principle is described in Figure 5.

At the physical layer, the bits affected by low noise levels can be corrected by the physical layer FEC, so that the related packets are passed to the higher layer as "correct." If the noise level exceeds the correcting capability of the physical layer, the received bit cannot be properly decoded, but the failure to decode can be usually detected with a very high reliability. Since erroneous packets are not propagated to the higher layers, we have an erasure channel. The system can use the redundancy packets to recover these erasures. By using maximum distance separable (MDS) codes, like the Reed-Solomon, it is possible to reconstruct the original information if at least k out of n packets are correctly received. Therefore, the receiver can cope with erasures, as long as they result in a total loss not exceeding h packets, independently from where the erasures occurred. LDPC codes and their derivations might be also used because of their low complexity and greater flexibility, thus permitting to encode larger files, although a small inefficiency, depending on the code design and typically around 5%–10%, will be taken into account.

If packet level FEC is implemented at IP or data link layer, very near to the physical channel, no change in the transport and network layers protocols and in the physical layer are necessary. This solution presents the additional advantage that it can be adapted to the propagation channel conditions

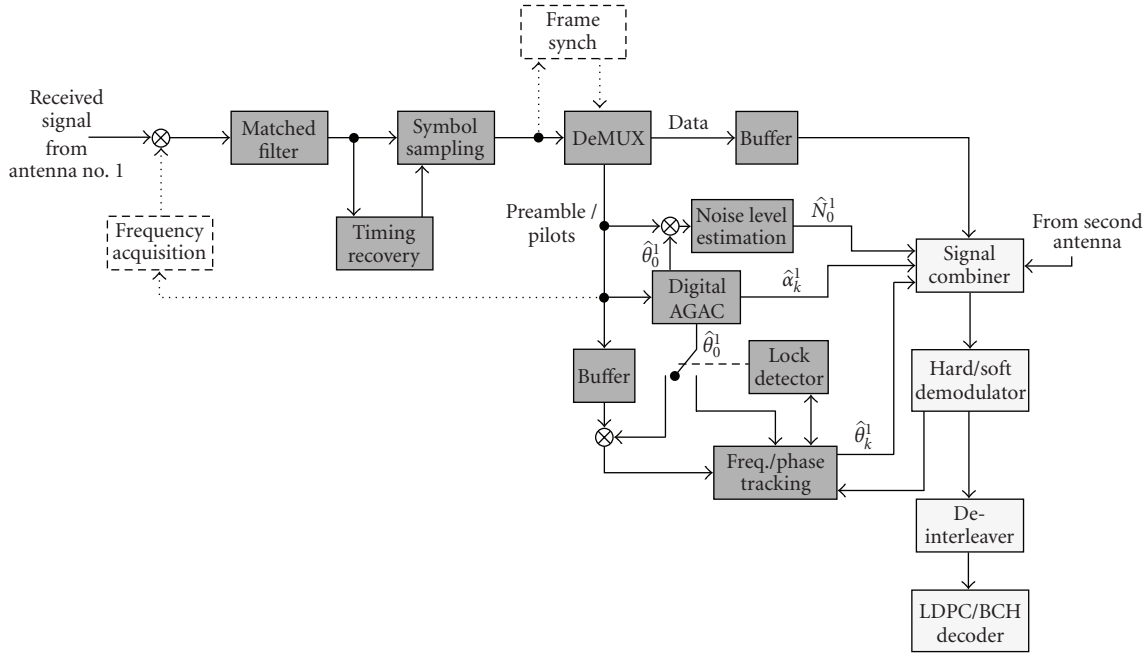

Figure 4: Receiver block diagram with antenna diversity.

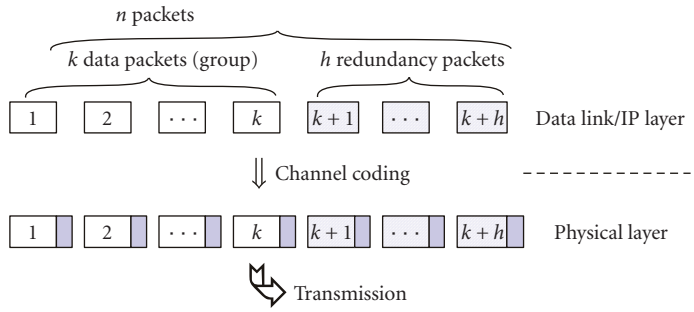

Figure 5: Packet level FEC principle.

by choosing n, so that the interleaver size is long enough to compensate the channel outages. However, different protection for individual transfers (e.g., specific files) is not possible (although different QoS classes may be supported), extra memory is required, and additional delays must be properly handled.

For the forward link, the usage of packet level FEC is especially powerful in allowing online variable coding approaches, which can be fine tuned in a closed-loop approach. Based upon the "history" of the link, appropriate redundancy can be easily added. Packet level FEC has then impact on different layers.

(i) The requirements on control loops can be lessened, for example, power control and or adaptive coding and modulation control, if a loss of up to h packets can tolerated.

(ii) The typical fade structure of a link can be measured and accordingly coding with the correct profile added.

(iii) Different QoS classes with different redundancy profiles can be supported. Furthermore, redundancy packets for low-priority traffic can be put in a special queue, which is served only if free capacity is available and, in turn, increased redundancy can be sent during handovers, minimizing the overall probability of lost packets.

(iv) Different IP-based access methods can be used in parallel, improving the link reliability if different redundancy is sent via different access methods.

4.2.2. The GSE-FEC method

When moving to the concrete applicability of this scheme to the scenario under consideration, even though the fact that IP packets have three sizes that are the most common ones, the fact that IP packet size can actually take any value up to a maximum value (typically 64 Kbytes) represents a clear

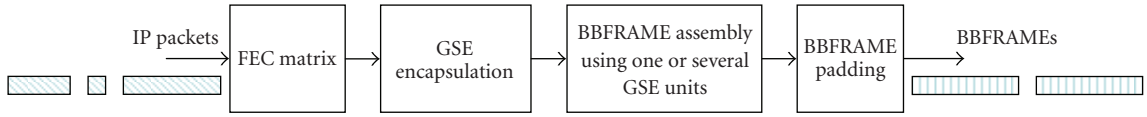

Figure 6: Steps involved in GSE-FEC.

difficulty in applying packet level FEC (PL-FEC). The fundamental difficulty comes from the fact that most codes take as input a fixed amount of data, from which they compute the redundancy bytes. As a given number of IP packets correspond to a variable amount of data depending of their sizes, codes needing a fixed amount of data cannot be directly applied. One possible solution is to use codes that can be easily adapted to different input sizes; however, this comes at the price of a much more complex encoding and decoding process. Another solution has been proposed in the DVB-H standard [16]. In this case, units of constant length are built by interleaving IP packets and, therefore, codes with fixed input size can be easily applied. It is worth noting that those units are not built by concatenating IP packets but by interleaving them. However, interleaving is this case must not be understood as it is typical in physical layer coding, where it means that data is written in one direction in a matrix and it is read in the orthogonal direction for transmitting. In PL-FEC, we understand interleaving as computing the redundancy in an orthogonal direction to the writing direction of the data; however, in this case the writing and reading directions coincide. This kind of interleaving is advantageous because the redundancy is computed across a large number of packets. Thus, a fade event may destroy one or several packets but not the majority of them, assuming that the system is well dimensioned, so the added redundancy can effectively help in recovering the destroyed packets.

DVB-H also provides a solution for encapsulating the coded IP packets for transmission over DVB-T. The solution is based on the use of multiprotocol encapsulation (MPE) combined with MPEG. Although it would be possible to adapt the same approach for DVB-S2, it presents a number of drawbacks, such as lack of flexibility, low encapsulation efficiency, delay constraints. A new encapsulation protocol call generic stream encapsulation (GSE) has been recently defined [17]. It is a very flexible protocol applicable to several physical layer standards. It overcomes most of the limitations of MPE-MPEG. GSE is especially suitable for transmitting IP packets through the generic stream interface mode of DVB-S2, and it has been proposed for the second generation of Terrestrial digital video broadcasting (DVB-T2) as well. GSE also efficiently supports the ACM functionalities of DVB-S2 and facilitates the provision of QoS guarantees because it reduces the constraints on the scheduling operation.

It can be deducted from the previous discussion that the implementation of PL-FEC consists of two main processes: the encoding the IP packets and, second, the encapsulation of the result of the encoding process in order to adapt it to the underlying transmission system. In DVB-H, the first process consists in arranging the IP packets in a matrix (hereafter called FEC matrix) and applying a Reed-Solomon code, while the second process employs MPE-MPEG. The whole implementation is called MPE-FEC in DVB-H. Our proposal for DVB-S2 is based on keeping the same first process as in DVB-H, whereas it employs GSE in the second process. This proposal for applying PL-FEC in DVB-S2 is named GSE-FEC.

A block diagram of GSE-FEC is depicted in Figure 6. The incoming IP packets are arranged in the so-called FEC matrix, where also the packet-level redundancy is added. The filling of the FEC matrix and the encoding are done in the same way as in DVB-H. For the sake of completeness, this will be briefly described below. Next, each IP packet is encapsulated using GSE, and this represents one of the novel aspects of our proposal. Each IP packet may be fragmented into several GSE units or it may also be sent unfragmented. Subsequently, the maximum number of GSE units that can be fitted inside a BBFRAME is concatenated and introduced in the BBFRAME. The size of the BBFRAME depends on the combination of coding rate and modulation scheme (MODCOD) adopted by the DVB-S2 modem, so the number of GSE units that can be concatenated also depends on the MODCOD. By making the GSE units small enough to have the required flexibility, but large enough in order not to penalize encapsulation efficiency, this method provides an easy mechanism to adapt the output of the packet-level FEC to the variations of the physical layer. Moreover, note that padding is not applied inside the GSE unit but only at BBFRAME level if the size of the BBFRAME does not coincide with that of the concatenation of the GSE units.

The IP packets are placed one after another along the columns of the FEC matrix, see Figure 7. Each IP packet may be split among two or more columns. Only the first block of the matrix, from column 1 to 191, can be filled in with IP packets. The second block of the matrix, from column 192 to 255, carries the redundancy information, which is computed by a Reed-Solomon (255,191) code applied to the first block on a row basis. Each column in the second block is encapsulated individually using GSE, whereas in the first block the GSE encapsulation is performed on an IP packet basis. In the baseline operation, padding is only applied in the first block to account for the fact that an additional IP packet may not be fitted without overrunning the 191 columns and all 64 redundancy columns are transmitted. The code can be made weaker (i.e., with higher rate) by puncturing some of the redundancy columns, which are then not transmitted and are considered as unreliable bytes in the decoding process. The code can also be made more robust (i.e., with lower rate) by padding with zeros columns in the first block and, hence, leaving less space for IP packets. The padded columns are not transmitted but they are used in the encoding process. In the decoding process, they are considered as reliable.

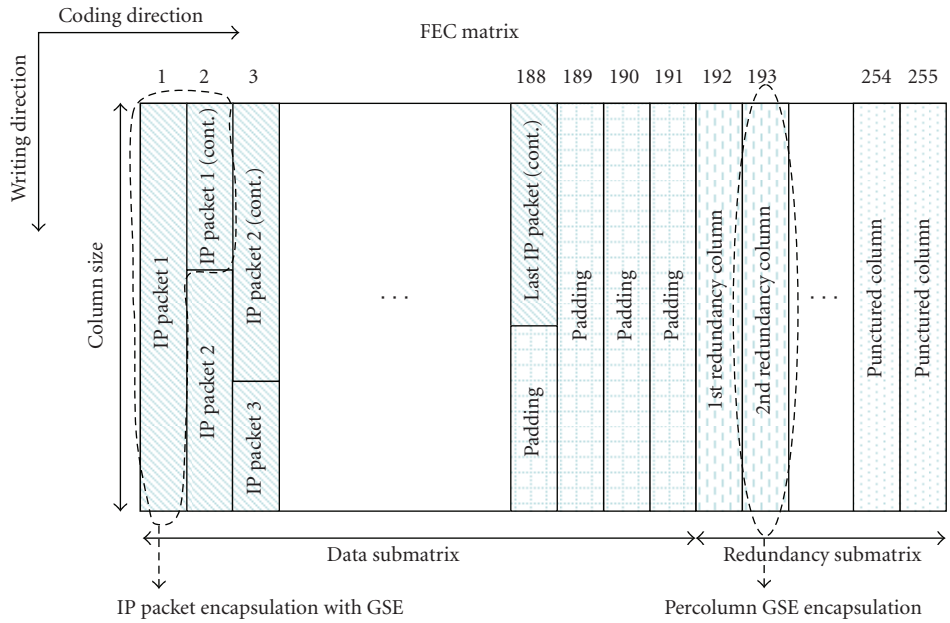

Figure 7: Arrangement of IP packets for FEC encoding.

After GSE encapsulation, the GSE packets are introduced in BBFRAMEs and transmitted. On the receive side, erroneous BBFRAMEs are detected by checking the CRC. The receiver reconstructs the FEC matrix and marks any column that is totally or partially received by means on an erroneous BBFRAME as unreliable. Finally, if the reconstructed FEC matrix has no more than 64 unreliable columns, the code can correctly compute all bytes in the matrix. If there are more than 64 unreliable columns, the code cannot correct anything, and only those columns received by means of correct BBFRAMEs will be correct.

5. SIMULATION SCENARIOS

In the following, the simulation platforms used to evaluate the performance of DVB-S2 with advanced fade countermeasures in the railway environment as described in Section 3 are duly detailed.

5.1. Advanced physical layer simulation platform

To cover a rather large set of spectral efficiency, four MODCODs have been considered: 1/2-QPSK, 2/3-8PSK, 3/4-16APSK, and 5/6-16APSK. The LOS channel condition (Rice factor equal to 17.4 dB) and the train speed equal to 300 km/h have been simulated. Equally spaced power arches with a separation of 50 m have been included in some scenarios, with a duty cycle of 1%, corresponding to a width of 0.5 m in accordance with Figure 2. The symbol rate was fixed to 27.5 Mbaud.

The considered DVB-S2 physical layer transmitter [2] is depicted in Figure 8. A continuous stream of MPEG packets passes through the mode adaptation which provides input stream interfacing. This data flow is passed to the merger/slicer that, depending on the applications, allocates a number of input bits equal to the maximum data field capacity. In this way, user packets are broken in subsequent data fields, or an integer number of packets are allocated in it. Then, a fixed length base-band header (BBHEADER) of 80 bits is inserted in front of the data field, describing its format. For example, it reports to the decoder the input streams format, the mode adaptation type and the roll-off factor. The efficiency loss introduced by this header varies from 0.25% to 1% for long and short codeword lengths, respectively. The role of stream adaptation is to provide padding when needed, in order to complete a constant length frame, and scrambling. Padding is applied when the user data available for transmission are not sufficient to completely fill a BBFRAME, or when more than one packet have to be allocated in a BBFRAME. The built frame is randomized using a scrambling sequence generated by the pseudorandom binary sequence described by the polynomial $(1 + X^{14} + X^{15})$. After this scrambling, each BBFRAME is processed by the forward error correction (FEC) encoder which is carried out by the concatenation of a Bose-Chaudhuri-Hocquenghem (BCH) outer code and an LDPC inner code. Available code-rates for the inner code are 1/4, 1/3, 2/5, 1/2, 3/5, 2/3, 3/4, 4/5, 5/6, 8/9, and 9/10. Depending on the application area, codewords can have length $N_{\mathrm{LDPC}} = 64800$ bits or 16200 bits. In the following, the case of 64800 bits is considered. Regarding the modulation format, each coded BBFRAME can be mapped onto QPSK, 8PSK, 16APSK, or 32APSK constellations. Modulated streams enter in the physical layer framing where physical layer signalling and pilot symbols are inserted. For energy dispersal, another scrambling sequence is applied to the entire physical layer frame (PLFRAME). The system has been designed to provide a regular PLFRAME structure, based on slots of $M = 90$ modulated symbols, which allow

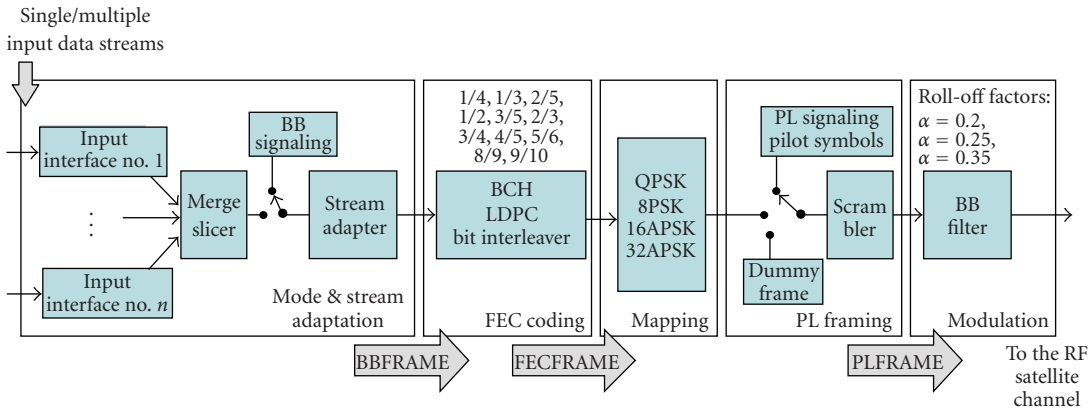

Figure 8: DVB-S2 physical layer transmitter block diagram (taken from [2]).

reliable receiver synchronization on the FEC block structure. The first slot, PLHEADER, is devoted to physical layer signalling, including start-of-frame (SOF) delimitation and MODCOD definition. Receiver channel estimation is facilitated by the introduction of a set of $P = 36$ pilot symbols, that are inserted every 16 slots. In addition, a pilotless transmission mode is also available, ensuring greater system capacity. Finally, for shaping purposes, a squared-root raised cosine (SRRC) filter with variable roll-off factors (0.2, or 0.25, or 0.35) is considered. To cope with the intrinsic nonlinearity of the on-board high power amplifier (HPA), a purposely designed predistortion technique is considered. In particular, a fractional predistortion technique based on a lookup table (LUT) approach is considered which operates right after the shaping filter [18]. The fractional predistorter, which is a digital waveform predistorter, acts on the signal samples for precompensating the HPA AM/AM and AM/PM characteristics and mitigating the impact of non linear distortion. In particular, the signal is processed by means of the LUT, which stores the inverted HPA coefficients computed offline through analytic inversion of a proper HPA model. The steps needed to obtain LUT coefficients are the following: *HPA model selection, parameter extrapolation, analytical model inversion, and LUT construction*. Regarding the first step, a simple yet robust empirical model is the classic Saleh model [18]. Given the measured HPA characteristics, the second step can be performed by minimizing the energy of the difference between the modelled and the experimental HPA curves (MMSE criterion). These parameters are then applied to the analytically inverted characteristics, so as to obtain the analytical predistortion transfer function. The last step is the quantization of the analytical curve in order to store it into the LUT. The adopted strategy is linear in power indexing, that is, table entries are uniformly spaced along the input signal power range, yielding denser table entries for larger amplitudes, where nonlinear effects reside.

The proposed digital receiver architecture is depicted in Figure 4. In particular, several subsystems are present in order to coherently demodulate and combine the received signals. The first coarse correction regards the carrier frequency, which allows match filtering with minimal intersymbol interference regrowth; then the subsequent block deals with clock recovery for timing adjustment, performed by a digital interpolator. The demultiplexer is used to separate pilots from data symbols in a PLFRAME. The pilot symbol stream is used by the following four subsystems: the noise level estimator, the digital automatic gain and angle control (AGAC), the block in charge of tracking the residual frequency offset and carrier phase, and finally the coarse frequency acquisition loop (not performed). On the other path, the data symbols, softly combined with the last equation of Section 4.1, feed the hard/soft demodulator. The demodulator provides the hard decisions on data symbols as a feed-back for carrier frequency and phase tracking, and computes the soft initial a posteriori probability (APP) on the received information bits. Finally, the APPs are deinterleaved and given to the LDPC-BCH decoder. As far as frame synchronization and frequency acquisition are considered, that is, dashed white blocks in Figure 4, they are not considered in the simulation chain because the receiver behaviour is assessed during steady state.

5.2. Packet level coding simulation platform

A simulation platform to analyze the performance of GSE-FEC has been developed. Given that this performance assessment entails many layers, in particular, from the physical to the network layers, of the protocol stack, a modular approach has been considered as the only feasible way to develop the platform. The physical-layer simulator described in the previous section interfaces with the packet-level simulator shown in Figure 9. This takes as input a stream of IP packets and applies the GSE-FEC encoding technique as described above, generating a sequence of BBFRAMEs. At this point, the output of the physical-layer simulator is used to mark the BBFRAMEs as correctly or wrongly received. Next, the GSE-FEC decoding process is applied. The effect of the BBFRAMEs on the GSE units and subsequently on the columns of the reconstructed FEC matrix is calculated. Then, the correction capability of the Reed-Solomon code is taken into account to eliminate, if possible, the unreliable columns

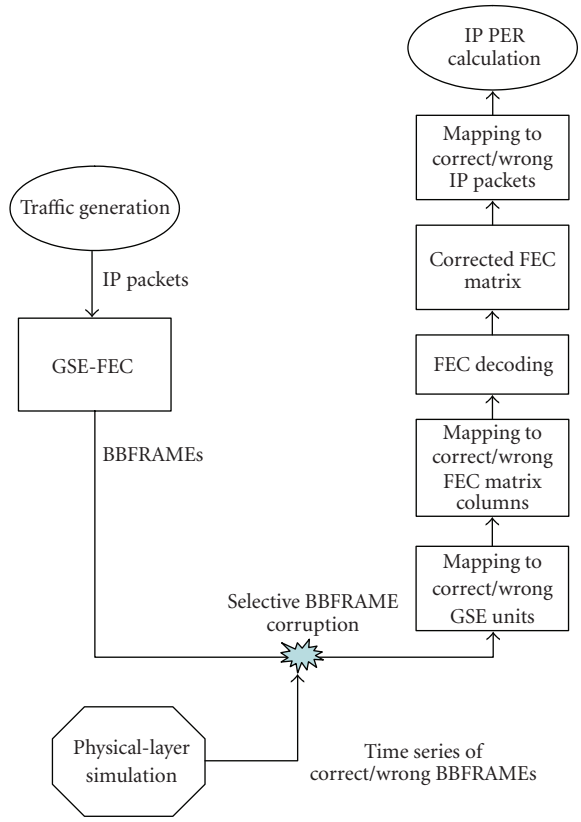

Figure 9: Simulation platform at IP-BBFRAME level.

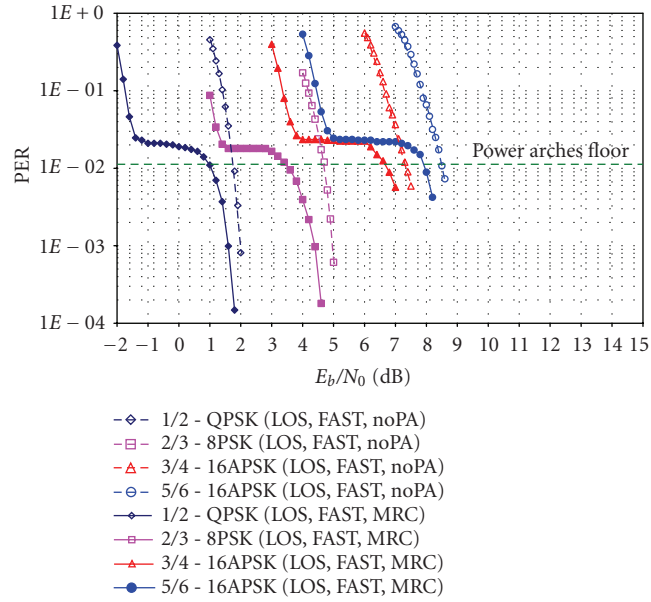

Figure 10: MRC performance in LOS channel condition and train speed equal to 300 km/h.

of the FEC matrix. Finally, the list of IP packets affected by the unreliable columns (an IP packet is considered wrong if any part of it falls inside an unreliable column which cannot be corrected) is obtained and the packet error rate (PER) at IP level is computed.

The packet-level simulator is useful to assess very quickly the performance of different parameter configurations of the GSE-FEC since different combinations can be simulated without the need of repeating the time-consuming physical layer simulations. The main parameters of GSE-FEC to be designed are the following:

(i) size of the columns of the FEC matrix,
(ii) size of GSE units,
(iii) number of padding columns in the first part of the FEC matrix,
(iv) number of punctured redundancy columns.

The effect of varying some of these parameters will be shown in the numerical results section.

6. RESULTS

6.1. Antenna diversity

Numerical results have been obtained by considering the entire transmit-receive chain described in Section 5.1. The introduction of the second receiving antenna adopting the MRC technique is reported in Figure 10. The most important result is that the MRC solution completely eliminates the error floor with respect to the single antenna case (see for comparison Figure 3). Secondly, it will be observed that instead of a constant 3- dB gain for all E_b/N_0 values, three different working regions can be distinguished. In particular, BBFRAME error rates curves are characterized by two waterfall regions separated by a short floor. This unexpected behaviour has a theoretical explanation that has been treated in details in [14]. Here, we limit the discussion to a numerical example. Let us consider MODCOD = 1/2-QPSK and a working $E_b/N_0 = 0$ dB, when a PA blockage event occurs, the "nonobscured" antenna has not a sufficient SNR to reliably decode the received MPEG packets, thus generating an error floor at that E_b/N_0. The second waterfall region starts only for E_b/N_0 values larger than 1 dB, when, as a matter of fact, a single antenna receiver has sufficient margin to correctly decode. This consideration can also be extended to all other MODCOD configurations. Notably, the short floor value is twice the floor value obtained with one receiving antenna; this is determined by the fact that there are two blockage events between two consecutive PA, that is, one per receiving antenna.

6.2. Packet level FEC

The objective of the following analysis is twofold: first, to provide a guideline for an appropriate choice of the column size of the FEC matrix, which is the key parameter in the GSE-FEC method; second, to analyze the performance of GSE-FEC under various configurations. In all cases, a scenario with line-of-sight propagation has been used.

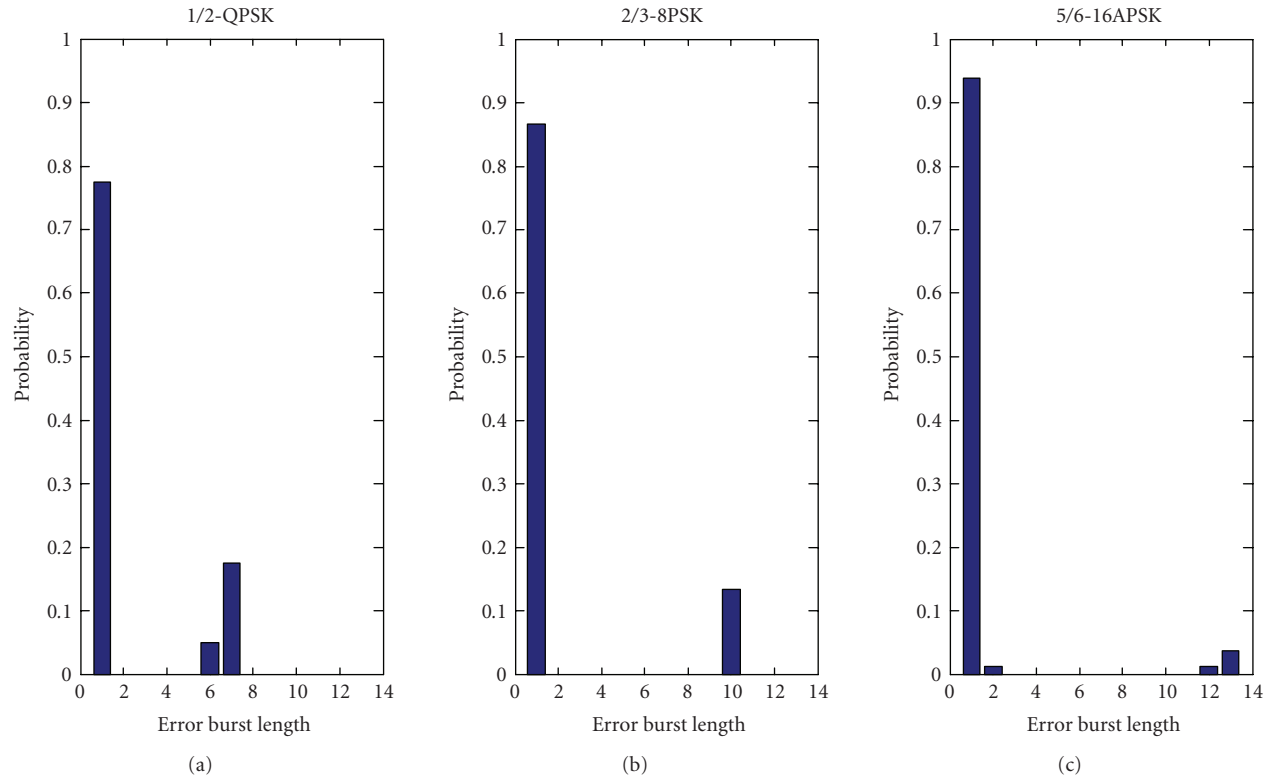

Figure 11: Histogram of the BBFRAME error burst length for two different MODCOD modes and target BBFRAME error rate equal to 0.02.

6.2.1. Dimensioning the FEC matrix

First of all, it is worth remarking that the appropriate size of the FEC matrix depends on the length of the bursts of erroneous BBFRAMEs. It is clear that longer bursts will require larger FEC matrices to avoid that the number of wrong columns exceeds the correction capability of the code. Therefore, the design of the height of the FEC matrix should be derived from an analysis of the length of the error bursts. Figure 11 shows the histogram of the length of the bursts for some particular MODCOD modes for the scenario described above. In all modes besides the two shown in Figure 11, it is observed that the distribution is bimodal. The bursts of short length (typically between 1 and 4 BBFRAMEs) are due to random errors caused by noise, whereas the rest of bursts are caused by the power arches. Second, the higher the modulation order, the longer the error bursts produced by power arches are. This is justified by the fact that according to the DVB-S2 standard, BBFRAMEs are coded and converted into FECFRAMEs, which have constant length in bits regardless of the used modulation [2]. The bits in the FECFRAME are transformed by the modulator into bytes in the PLFRAMEs. Higher modulations need fewer symbols and, hence, less time to transmit an FECFRAME. The duration of the fade event caused by a power arch only depends on the speed of the train, which we have considered to be 300 km/h throughout the rest of the paper. Therefore, the shorter the PLFRAME, the more PLFRAMEs and hence BBFRAMEs are affected by each power arch.

In order to present the procedure to compute the column size of the FEC matrix, we consider a numerical example. We use for instance the least efficient MODCOD, that is, 1/2-QPSK. It can be seen in Figure 11 that the maximum error burst length due to power arches is 7 BBFRAMEs. In this MODCOD, each BBFRAME has a data field of length 32128 bits [2], which is equal to 4016 bytes. Therefore, a burst of 7 BBFRAMES corresponds to 28112 bytes. We consider that this amount of bytes should correspond to less than 30 columns in the FEC matrix. The value of 30 has been chosen arbitrarily. It is nevertheless a reasonable number since the objective is to leave a margin with respect to the 64 columns that the code can correct (assuming no puncturing) so as to be able to cope with errors caused by noise as well. Therefore, the column size of the FEC matrix should fulfil

$$30L_c \geq 28112 \Longrightarrow L_c \geq 938 \text{ bytes}, \tag{7}$$

where L_c is the number of rows (i.e., the length of each column) of the FEC matrix in bytes. In the previous computation, we have not taken into account the overhead introduced by GSE since it is small and we are only interested in obtaining an approximate value for the column size. If the same calculation is repeated for the most efficient MODCOD, that is, 5/6-16APSK, the result is $L_c \geq 2912$ bytes. The

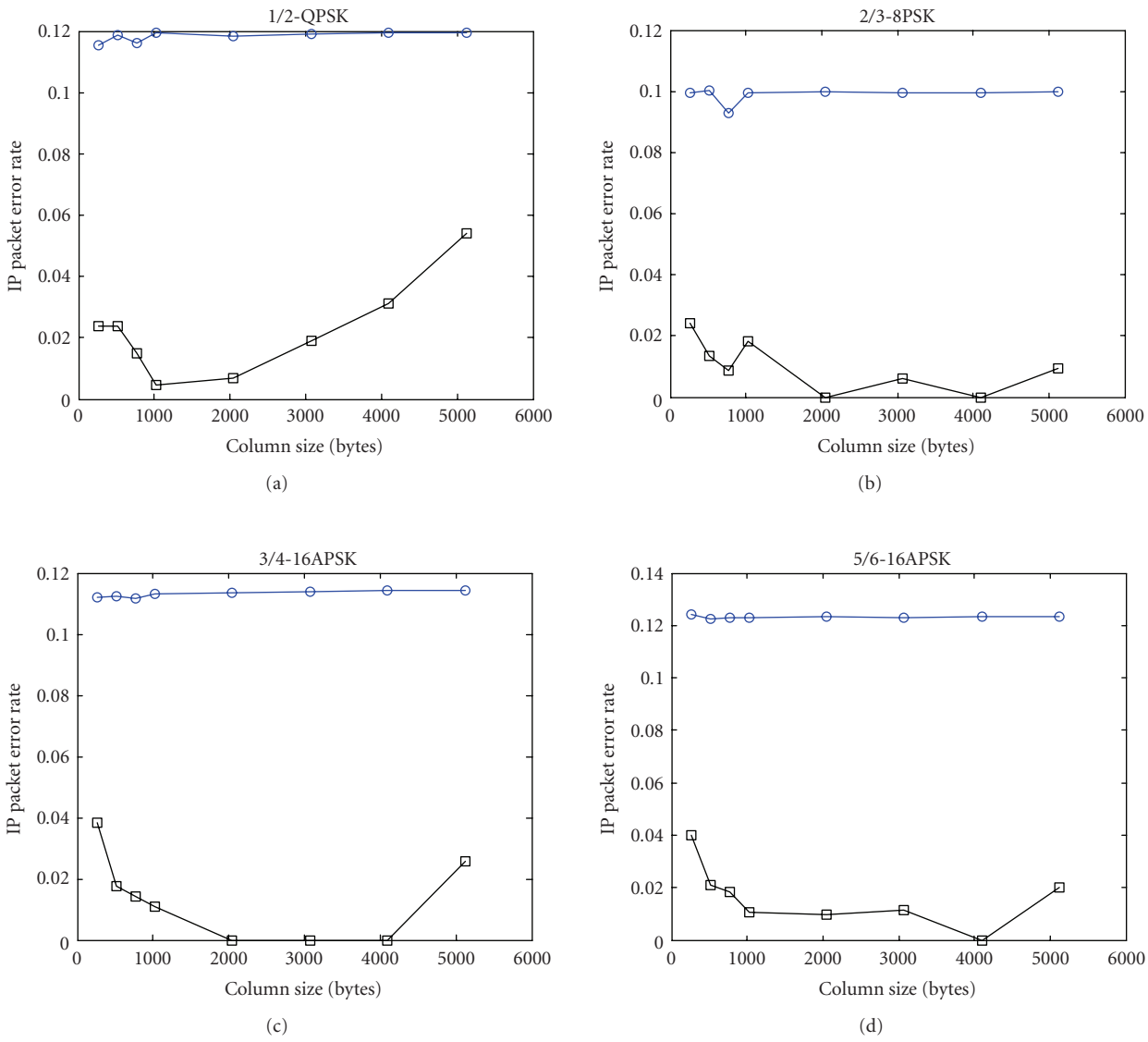

Figure 12: Comparison of the IP packet error rate for different ACM modes in a channel with BBFRAME error rate equal to 12% (circles → results without any kind of PL-FEC, squares → results with GSE-FEC).

results for the intermediate MODCODs, 2/3-8PSK and 3/4-16APSK, are 1790 and 2618 bytes, respectively.

We conclude from this discussion that the appropriate size of the FEC matrix strongly depends on the error burst length caused by the power arches, which in its turn depends on the train speed. The lower the train speed is, the longer the bursts are and the taller the FEC matrix must be. However, the size of the FEC matrix cannot be increased arbitrarily because it has an impact on the delay of GSE-FEC process and, on top of that, because more errors due to noise appear inside the FEC matrix. These errors may risk the correction capability of the code, as will be seen below. Therefore, the performance of GSE-FEC may be limited for low train speeds since it is not possible to combat simultaneously very long error bursts due to power arches and a large amount of random errors due to noise.

6.2.2. *Performance analysis*

Dependence on the size of the FEC matrix

The IP packet error rate as a function of the column size for different MODCODs is shown in Figures 12 and 13. The considered columns sizes and the corresponding number of GSE units used to encapsulate each RS redundancy column are listed in Table 2. The number of GSE units per column has been selected in such a way that the size of the units is small enough to limit the amount of padding in the BBFRAMEs, but large enough not to penalize encapsulation efficiency (encapsulation efficiency is out of the scope of this work and will be analyzed in a follow-on paper). A fixed IP packet length equal to 576 bytes has been considered.

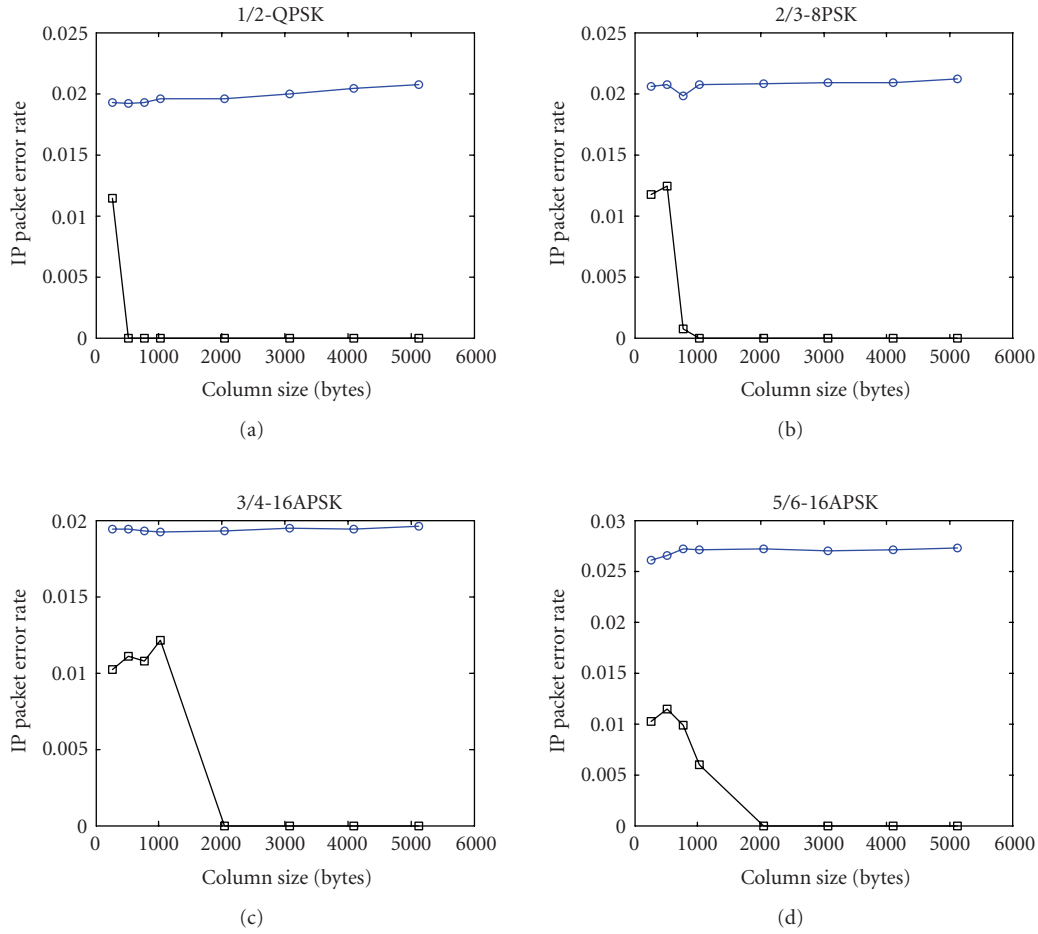

Figure 13: Comparison of the IP packet error rate for different ACM modes in a channel with BBFRAME error rate equal to 2% (circles → results without any kind of PL-FEC, squares → results with GSE-FEC).

Figures 12 and 13 also compare the results obtained when GSE-FEC is used and when no packet-level FEC is applied. The baseline GSE-FEC is employed, that is to say, no additional padding has been used in the first 191 columns and no puncturing of the last 64 columns has been performed. The case of no packet-level FEC follows the same architecture as for GSE-FEC, depicted in Figures 6 and 7. The difference is that the 255 columns of the FEC matrix are filled with IP packets and no redundancy is introduced into it. Figure 12 was obtained when the physical-layer simulator was tuned to provide a BBFRAME error rate around 0.12, whereas Figure 13 was obtained for a value of 0.02.

In the case of no packet-level FEC, the IP PER is almost insensitive to changes in the column size and its value is very close to the BBFRAME error rate, as expected. It is very interesting to observe that the proposed scheme, GSE-FEC, effectively reduces the IP PER and, in many configurations, the IP PER is exactly zero.[3] This means that, in those cases, all IP packets were correctly received in spite of the fact that the BBFRAME error rate is higher than 10%.

For small column sizes, the IP PER decreases as the column size increases. This behaviour is in line with the discussion at the beginning of this section: when the FEC matrix is too small, a power arch causes errors in a portion of the matrix that is too large to be corrected by the code. The IP PER decreases until it reaches a minimum, which is attained at a column length that is well approximated by the previous back-of-the-envelope calculations. If the column length is increased further, the IP PER increases because the correction capability of the code is fixed and equal to 64 columns, but the size of the FEC matrix becomes larger and, hence, the number of errors due to noise increases. This behaviour is visible in Figure 12, but not in Figure 13. The reason is that the later figure corresponds to a scenario with very high signal-to-noise ratio, and BBFRAME errors are almost only caused by power arches.

Dependence on the IP packet length

The effect of different IP packet lengths is shown in Figure 14. In this case, the column size of the FEC matrix is fixed

[3] Note that the simulation duration was equal to 5000 BBFRAMEs, so we can only say that the IP PER is not worse than 2×10^{-5}.

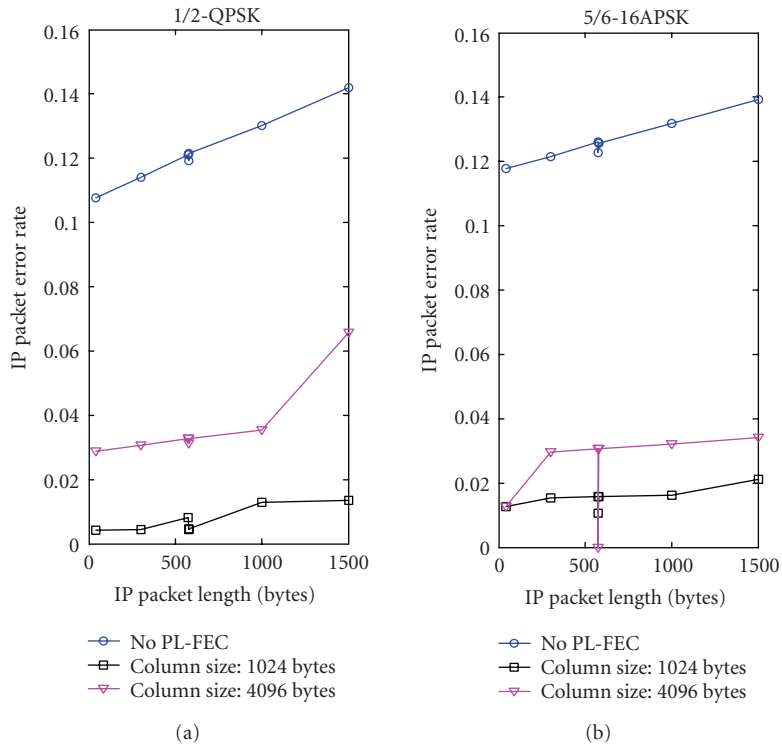

Figure 14: Dependence of the IP packet error rate with the IP packet size for two column sizes (1024 and 4096 bytes) and two MODCOD modes (1/2-QPSK and 5/6-16APSK).

and equal to 1024 or 4096 bytes. The general trend is that the IP PER slightly increases as the IP size increases. There are however some lengths, such as 576 bytes, that are especially favourable. This happens because for those lengths an integer number of IP packets fit in an integer number of columns of the FEC matrix. For instance, it is fulfilled that $576 \times 16 = 1024 \times 9$, which means that 16 IP packets of length 576 bytes fit in 9 columns of length 1024 bytes. As this perfect fitting reduces the ratio of IP packets that are split across two columns, the number of IP packets corrupted by a wrong column is also reduced on average. If the length of IP packets follows a certain distribution, as it happens with real traffic, the IP PER can be obtained by computing an average of the values shown in Figure 14. This average would be computed by weighting the IP PER for a given length by the frequency of occurrence of that length.

Conclusions on GSE-FEC results

The analysis of the GSE-FEC and the corresponding numerical results has shown that the column size is a key design parameter. Long columns appropriate to obtain low IP PER when the duration of the fade events caused by power arches is large (e.g., when the train is moving slowly) or when very spectrally efficient MODCODs are used; but this comes at the price of a large encoding and decoding delay, and an increased sensitivity to random BBFRAME errors caused by noise and interference. Therefore, the column size must be selected as the result of a tradeoff between competing goals; it is not possible to propose a single value appropriate for all scenarios. We consider that the column size must be an adaptive parameter, which is changed in response to variations of the propagation conditions, train speed, and so forth. This adaptation would constitute an example of cross-layer optimization, whereby a link layer parameter (i.e., the column size of the FEC matrix) is adapted as function of the physical-layer conditions. The padding and puncturing of columns in the FEC matrix are other degrees of freedom that can be exploited in the parameterization of GSE-FEC. A detailed analysis of these aspects is a subject for further research.

6.3. Comparative analysis

As it can be seen from the results presented in the last two sections, very satisfactory results to ensure reliable reception can be obtained with both techniques. In the case of antenna diversity, this does not penalize the overall system efficiency, although some additional complexity in the receiver implementing the MRC scheme will be accounted for. However, the main issue to be addressed in the practice is represented by the installation of two antennas. Many experiments and trials have shown that this is a very critical point, since antennas suitable for installation on trains are subject to very strict requirements in terms of pointing accuracy, size, and robustness against mechanical vibrations, wind, pressure gradients when entering or exiting a tunnel, and so forth. With current antenna technologies, a relatively high failure rate

Table 2: Parameters of the GSE-FEC algorithm.

FEC-matrix column size (bytes)	256	512	768	1024	2048	3072	4096	5120
GSE units per column	1	1	1	2	2	3	4	5

of mechanical components included in the antenna platform has to be expected. Furthermore, train operators are extremely keen on keeping the installation and maintenance procedures as simple as possible. For all these reasons, additional countermeasures must be also investigated as possible complement to the presence of two antennas (e.g., in case one antenna suddenly breaks and no immediate replacement is possible).

Although it has been shown that the dimensioning of packet level FEC is a complex task, that will be carried out following a cross-layer approach, the results presented in the previous section confirm that also this technique, if properly designed, can guarantee reliable reception at the expenses of a limited increase in the system complexity and overhead. The concrete solution presented in this paper has been especially devised taking into account the architectural constraints introduced by the latest encapsulation scheme (GSE) currently being proposed for future DVB systems. Clearly, packet level FEC results in a reduction of the overall spectral efficiency of approximately 33% with the adopted RS code, partially compensated by the migration to a more efficient encapsulation scheme such as GSE.

7. CONCLUSIONS

To conclude, two countermeasures are thoroughly analyzed in this paper: antenna diversity and a packet-level forward error correction mechanism especially tailored to DVB-S2, named GSE-FEC. Simulations have shown the excellent performance of both approaches, while they have complementary features in terms of hardware complexity, delay, and bandwidth efficiency. Generally speaking, the results in this paper show that effective countermeasures to compensate the impairments of the railroad satellite channel are possible and can be integrated into the existing DVB-S2 standard with a limited to moderate impact on the receiver design and on the system complexity. In fact, to support antenna diversity, the receiver structure will be modified as depicted in Figure 4, whereas for packet level FEC a software implementation may be considered.

Further topics to be addressed in order to conclude the analysis of the forward link are the following:

(i) cross-layer optimization of all the relevant parameters (MODCODs and GSE-FEC), taking also into account nLOS channel conditions and the usage of ACM to compensate for slower fades due to atmospherical effects,

(ii) inclusion of mechanizm(s) to support QoS and study of their integration and interaction with the proposed GSE-FEC scheme.

ACKNOWLEDGMENT

This work was supported and partially funded by SatNEx, the Satellite Communications Network of Excellence (www.satnex.org), FP6 Contract IST-507052.

REFERENCES

[1] EN 300 421 v1.1.2: Digital Video Broadcasting (DVB); Framing structure, channel coding and modulation for 11/12 GHz satellite services.

[2] ETSI EN 302 307 v1.1.1: Digital Video Broadcasting (DVB): Second generation framing structure, channel coding and modulation system for Broadcasting, Interactive Services, News Gathering and other broadband satellite applications.

[3] ETSI EN 301 790 v1.4.1: Digital Video Broadcasting (DVB): Interaction channel for satellite distribution systems.

[4] ETSI TR 101 790 v1.3.1: Digital Video Broadcasting (DVB): Interaction channel for satellite distribution systems; Guidelines for the use of EN 301 790.

[5] ETSI EN 302 304 v1.1.1: Digital Video Broadcasting (DVB); Transmission System for Handheld Terminals (DVB-H).

[6] S. Scalise, R. Mura, and V. Mignone, "Air interfaces for satellite based digital TV broadcasting in the Railway environment," *IEEE Transactions on Broadcasting*, vol. 52, no. 2, pp. 158–166, 2006.

[7] E. Lutz, M. Werner, and A. Jahn, *Satellite Systems for Personal and Broadband Communications*, Springer, New York, NY, USA, 2000.

[8] S. Scalise, H. Ernst, and G. Harles, "Measurement and modelling of the land mobile satellite channel at Ku-band," to appear in *IEEE Transactions on Vehicular Technology*.

[9] E. Kubista, F. P. Fontan, M. A. V. Castro, S. Buonomo, B. R. Arbesser-Rastburg, and J. P. V. Polares Baptista, "Ka-band propagation measurements and statistics for land mobile satellite applications," *IEEE Transactions on Vehicular Technology*, vol. 49, no. 3, pp. 973–983, 2000.

[10] A. Benarroch and L. Mercader, "Signal statistics obtained form a LMSS experiment in Europe with the MARECS satellite," *IEEE Transactions on Communications*, vol. 42, no. 2–4, pp. 1264–1269, 1994.

[11] G. Sciascia, S. Scalise, H. Ernst, and R. Mura, "Statistical characterization of the railroad satellite channel at Ku-band," in *Proceedings of the International Workshop of Cost Actions 272 and 280*, Noordwijk, The Netherlands, May 2003.

[12] S. Scalise, O. Lücke, and E. V. Torralbo, "A link availability channel model for the railroad satellite channel," in *Proceedings of 24th AIAA International Communications Satellite Systems Conference (ICSSC '06)*, vol. 1, pp. 305–317, San Diego, Calif, USA, June 2006.

[13] S. Cioni, G. E. Corazza, and A. Vanelli-Coralli, "Antenna diversity for DVB-S2 mobile services in Railway environments," to appear in *Journal of Satellite Communications and Networks*, special issue on ASMS Conference.

[14] S. Cioni, M. Berdondini, G. E. Corazza, and A. Vanelli-Coralli, "Antenna diversity for DVB-S2 mobile services in Railway environments," in *Proceedings of the 3rd Advanced Satellite Mobile Systems (ASMS) Conference*, Herrsching am Ammersee, Germany, May 2006.

[15] S. Cioni, A. Vanelli-Coralli, C. Párraga Niebla, S. Scalise, G. Seco Granados, and M.A. Vázquez Castro, "Antenna diversity and GSE-based packet level FEC for DVB-S2 systems in Railway scenarios," in *Proceedings 25th AIAA International*

Communications Satellite Systems Conference, Seoul, South Korea, April 2007.

[16] ETSI TR 102 377 v1.2.1: Digital Video Broadcasting (DVB); DVB-H Implementation Guidelines.

[17] DVB Blue Book A116 - Generic Stream Encapsulation Specification. http://www.dvb.org/technology/bluebooks/a116.tm3762r1.gbs0436r10.GSE_spec.pdf.

[18] P. Salmi, M. Neri, and G. E. Corazza, "Design and performance of predistortion techniques in Ka-band satellite networks," in *Proceedings of the 22nd AIAA International Communications Satellite Systems Conference and Exhibit (ICSSC '04)*, vol. 1, pp. 281–291, Monterey, Calif, USA, May 2004.